

A CA/MC model for the simulation of grain structures in solidification processes

TONGMING WANG, JUNZE JIN, XIANSHU ZHENG

Research Center of Foundry Engineering, Dalian University of Technology,
Dalian 116024, People's Republic of China

E-mail: tmwang@mpd.ams.eng.osaka-u.ac.jp

A CA/MC model is established to simulate the grain structures of solidification processes. It first describes the envelop of grain by using Cellular Automaton technique, then the interior of grain is corrected by Monte Carlo method. In this paper, solute field is calculated in microscopic scope, and the solute redistribution in solid/liquid interface is calculated by using Actual Solute Partition Coefficient model. The CA/MC model is applied to simulate the microstructure evolution of Al-4.5% (mass) Cu alloy in water-cooled Cu mould. It shows that the simulation result is agreement with that obtained experimentally.

© 2002 Kluwer Academic Publishers

1. Introduction

In recent years, many models used for structure simulation have been developed. For example, Wang and Beckermann developed the Multiscale and Multiphase model, which is based on the volume averaging technique [1–3]. Brown, Spittle, Zhu and Smith established Monte Carlo (MC) method based on the law of the lowest energy [4–6]. Rappaz and Gandin developed the Cellular Automaton (CA) technique to simulate structure formation [7], in which the physical mechanism of growth of dendritic grains is involved. Subsequently, a coupled Finite Element-Cellular Automaton model for the prediction of grain structure is developed by Rappaz *et al.* [8].

The aim of the present contribution is to present CA/MC model, which combines CA technique and MC method in an effective way. By CA/MC model, the evolution of amount, size and appearance of grains can be simulated better than those only by CA technique or MC method.

2. Heat flow calculation

Thermal field is the necessary data for the simulation of grain structures. In present study, thermal field at any moment is calculated by Alternant Explicit Difference (AED) method, which absorbs the advantage of Explicit Difference method and Implicit Difference method. Here, the latent heat released is calculated according to the solidification fraction f_S , which can be fed back from the results of structure simulation. The heat latent released in unit volume, \dot{q} , is given by

$$\dot{q} = \rho \cdot \Delta h \cdot \frac{\partial f_S}{\partial t} \quad (1)$$

where ρ is density, Δh is heat latent.

3. Solute calculation

In this paper, solute diffusion is calculated by the Direct Finite Difference method. In addition, a new model

based on structure simulation is proposed to calculate the solute redistribution in the solid/liquid interface. The rejected solute from the cell of phase change are calculated according to the actual solute partition coefficient k_a , and the cell which phase change occurred can be got by the structure simulation. It is because that solute calculation and structure simulation share the same meshes that are used for the microscopic simulation.

For a cell of phase change, the solute conservation equation is

$$\rho V_c \left(\omega_L + \sum_{i=1}^n \omega'_{Li} \right) = \rho V_c (\omega_S + \bar{\omega}'_L \cdot n) \quad (2)$$

where ω_L is the solute mass fraction before phase changing, and ω_S is the solute mass fraction after phase changing, $\sum_{i=1}^n \omega'_{Li}$ is the sum of solute mass fraction of all the liquid cells neighbor to the current cell, and n is the number of all the neighbor liquid cells, $\bar{\omega}'_L$ is the averaging solute mass fraction of all the neighbor liquid cells after phase changing, V_c is the volume of the current cell.

According to the definition of the actual solute partition coefficient, there is

$$k_a = \frac{\omega_S}{\bar{\omega}'_L} \quad (3)$$

Here, $\bar{\omega}'_L$ is taken as the solute mass fraction of liquid in the solid/liquid interface.

In addition, it should be pointed out that K_a is not equal to K_0 which is the solute equilibrium partition coefficient.

In the near equilibrium situation, k_a can be calculated by the Button model [9]

$$k_a = \frac{k_0}{k_0 + (1 - k_0) \exp\left(-\frac{R}{D_L} \delta\right)} \quad (4)$$

where, R is the solidification rate, δ is the thickness of diffusion boundary layer.

In the near rapid solidification situation, Aziz model is often used to calculate k_a [10]. For the step growth, there is

$$k_a = k_0 + (1 - k_0) e^{\left(-\frac{1}{\beta}\right)} \quad (5)$$

For the continuous growth, there is

$$k_a = \frac{\beta + k_0}{\beta + 1} \quad (6)$$

where $\beta = \frac{Rd}{D_L}$, D_L is the solute diffusion coefficient of liquid, d is the thickness of atom layer in the solidification direction, here it is equal to atom diameter approximately.

According to the Equations 2–4 or 5 or 6, the ω_S can be got. Then the rejected solute of the current cell when phase change occurs are given by

$$\Delta S = \rho V_c (\omega_L - \omega_S) \quad (7)$$

Then, the rejected solute, ΔS , are distributed to the neighbor liquid cells of the current cell according to the specific coefficient p_i : $p_i = \Delta T_i / \Delta T_{\text{sum}}$, ΔT_i is the temperature difference between one of the neighbor liquid cells and the current cell, ΔT_{sum} is the sum of all the temperature difference. The solute redistribution in the front of solidification is finished by this approach.

The solute calculation model above is well adapted for the numerical simulation.

4. Nucleation

A continuous nucleation distribution, $dn/d(\Delta T)$, can be used to describe the grain density increase, dn , which is induced by an increase in the under-cooling, $d(\Delta T)$. Therefore, the total density of grains, $n(\Delta T)$, which have been nucleated at a given under-cooling, ΔT , is given by the integral of this distribution [8]

$$n(\Delta T) = \int_0^{\Delta T} \frac{dn}{d(\Delta T')} d(\Delta T') \quad (8)$$

In the present work, two different Gaussian distributions are used to describe heterogeneous nucleation at the mould surface and in the bulk of the melt respectively. It is shown in Fig. 1. The total density of grains, $n(\Delta T)$ is then given

$$n(\Delta T) = \frac{n_{\text{max}}}{\sqrt{2\pi} \Delta T_\sigma} \int_0^{\Delta T} \times \exp\left[-\frac{1}{2} \left(\frac{\Delta T' - \Delta T_N}{\Delta T_\sigma}\right)^2\right] d(\Delta T') \quad (9)$$

where n_{max} is the number of original nucleation sites, ΔT_N , ΔT_σ are mean under-cooling and standard deviation respectively. If the extinction of nucleation sites

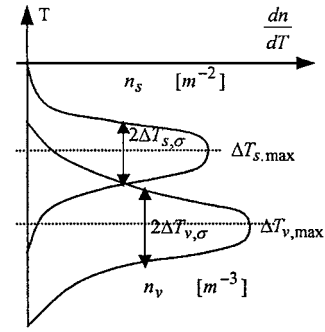


Figure 1 Nucleation site distributions for nuclei formed at the mould wall and in the bulk of the liquid.

by the growing grains is taken into account, then Equation 9 should be multiplied by $(1 - f_s)$.

5. Growth algorithm

In the present work, two different size meshes are respectively used for calculation of thermal field and simulation of grain structures. The larger one is called “element”, and the smaller one is called “cell”. In order to simulate the grain structures more easily, an effective data organization of cells is needed. The data organization of a cell is shown in Table I.

Before calculation, each cell is initialized by given a unique number. In addition, the nucleation mark is set “false”, and the value of crystal orientation is assigned “-1” which represents liquid. The temperature of each cell can be got from macro thermal field by rectangle interpolation.

Let consider first a cell generated by random sampling.

1. If the cell under-cooling, $\Delta T < 0$, nothing to do but continue to choose the next cell by random sampling.

2. If the cell is liquid, the nucleation calculation will be done. According to the nucleation model, there is

$$\begin{aligned} \delta n &= n[\Delta T + \delta(T)] - n(\Delta T) \\ &= \int_{\Delta T}^{\Delta T + \delta(T)} \frac{dn}{d(\Delta T')} d(\Delta T') \end{aligned} \quad (10)$$

where δn is the grain density increase in one time-step, and $\delta(T)$ is the under-cooling increase in one time-step.

TABLE I The data organization of a cell

Cell number
Temperature
Under-cooling
Concentration
Nucleation mark
Crystal orientation (integer)
Near mould mark
Material mark
Number of neighbor cells
Number of nucleation cell
Grain information (the radius of dendritic tip, the length of dendrite arm. etc.)

Then the nucleation probability p_n is given by

$$p_n = \delta n V_c \quad (11)$$

If $p_n > r$, r , is a random number ($0 \leq r \leq 1$), the cell's nucleation succeeds. This cell transforms from liquid to solid, a random integer (>0) which represents a certain crystal orientation is assigned for it, the nucleation mark is set "true", meanwhile, the calculation of solute redistribution is done for it.

3. If the cell is a nucleation site (the nucleation mark is "true"), the growth calculation is done for the grain. The radius and the velocity of dendritic tip can be given by KGT model, therefore, the length of dendritic arm, L , can be obtained and the grain information can be updated in current time-step.

4. If the cell is solid and some of its neighbor cells are still liquid, the entrapment of a neighbor liquid cell by the growing grain, which possesses of the current cell, can be done by using CAMC model. The procedure is detailed below.

The grain that possesses of the current cell is labeled "A". The envelop of grain A can be described by the following equation which is reported by Beckermann *et al.* [11].

$$\frac{X_{\text{tip}}}{R} = 0.668 \left(\frac{Z}{R} \right)^{0.859} \quad (12)$$

Or

$$X_{\text{tip}} = 0.668 R^{0.141} Z^{0.859} \quad (13)$$

The symbols in Equation 12 are shown in Fig. 2.

In order to establish the capture rule easily, the coordinate transformation is needed here. The coordinate origin is translated first to the nucleation site of grain A, and the coordinate system is rotated to make the coordinate axis coincide with the primary arms of grain A, as shown in Fig. 3.

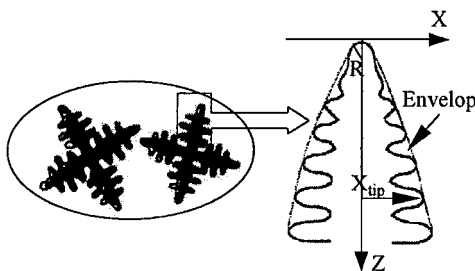


Figure 2 The dendritic envelop normalized by Beckermann.

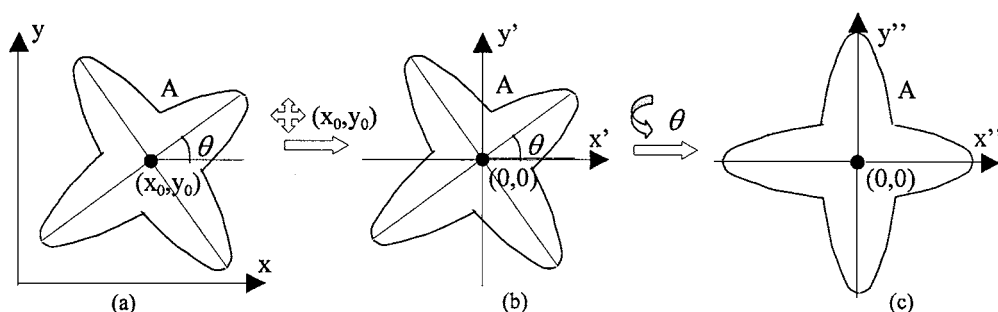


Figure 3 Coordinate transformation (a) originality (b) translation (c) rotation.

The corresponding mathematical manipulation is given by

Translate to (x_0, y_0) ,

$$\begin{aligned} x' &= x - x_0 \\ y' &= y - y_0 \end{aligned} \quad (14)$$

Rotate angle, θ ,

$$\begin{aligned} x'' &= x' \cos \theta + y' \sin \theta \\ y'' &= y' \cos \theta - x' \sin \theta \end{aligned} \quad (15)$$

At the base on the coordinate conversion, it is easy to judge whether a liquid cell is captured by grain A in current time-step. First, take into account the situation that the liquid cell is in the first quartile ($x_i'' \geq 0, y_i'' \geq 0$), as shown in Fig. 4. According to the Equation 13, for a liquid cell (x_i'', y_i'') , there is

(a)

$$\begin{aligned} Z &= L_1 - x_i'' \\ X_{\text{tip}} &= 0.668 \cdot R_1^{0.141} \cdot Z^{0.859} \end{aligned} \quad (16)$$

If $y_i'' \leq X_{\text{tip}}$, the liquid cell is captured by the dendritic arm "1".

(b)

$$\begin{aligned} Z &= L_2 - y_i'' \\ X_{\text{tip}} &= 0.668 \cdot R_2^{0.141} \cdot Z^{0.859} \end{aligned} \quad (17)$$

If $x_i'' \leq X_{\text{tip}}$, the liquid cell is captured by the dendritic arm "2".

If the situations of (a) and (b) are all false, the liquid cell is not captured by grain A. Otherwise, the liquid cell is in the envelop of grain A. The orientation of this liquid cell is given the same value of grain A. Meanwhile, the calculation of solute redistribution is done for it. If the liquid cell is in other quartile, the similar judgement can be done.

In addition, the other liquid neighborhood of the current cell e.g., the second- and third-nearest etc. are treated similarly by a recursive algorithm.

5. If the cell is solid and its neighbor cells are all solid, nothing to do but continue to choose the next cell by random sampling.

When all the cells have been chosen completely, the work of next time-step will begin. The growth algorithm

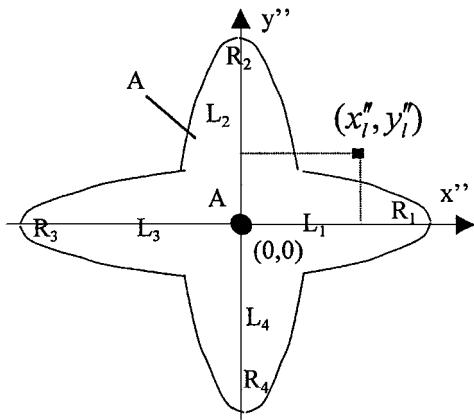


Figure 4 Diagram of relationship between liquid cell and grain.

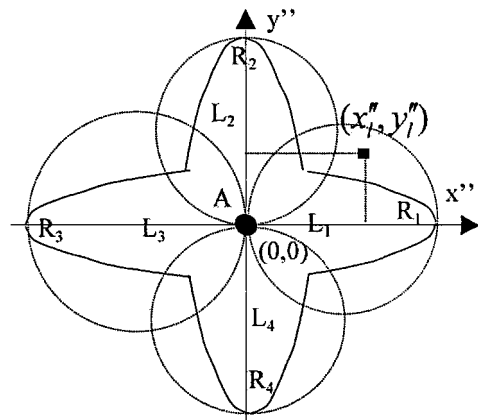


Figure 6 The area for MC correction growth.

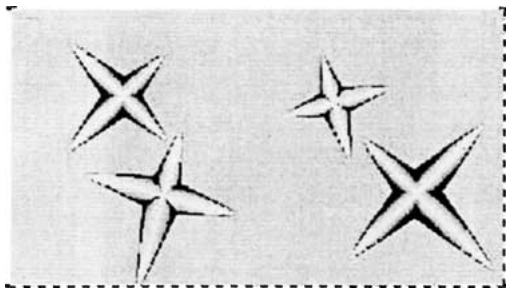


Figure 5 Grain images simulated by CA technique (Gradation represents solute concentration).

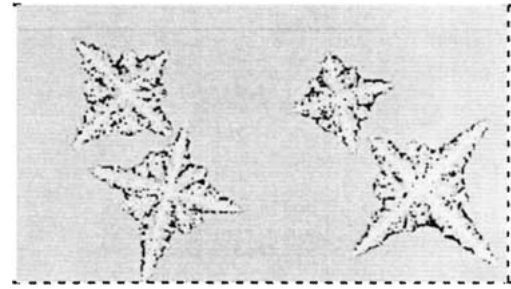


Figure 7 Grain images simulated by CA/MC model (Gradation represents solute concentration).

above has the essentials of CA technique. The difference to Rappaz's CA technique is the capture rule.

The CA technique presented here accounts for the growth kinetics of the dendritic tips, and for the preferential growth directions. The grain images simulated by this technique are shown in Fig. 5. It is noted that the grain images are slightly different from the normal grains obtained experimentally. The reasons are that the current CA technique only adopts a deterministic equation to describe the grain shape, and the equation is limited ($Z \gg R$) which does not adapt to the dendritic tip, in addition, it does not account for the branching mechanisms of dendrite.

In order to make up the deficiency of CA technique above, MC method is used to correct the growth of grain interior. MC also called random simulation method based on the theory of probability statistics. The MC method doesn't only account for the effects of bulk free energy and interfacial energy but also reflects the random procedure and branching mechanisms of grain growth.

When establishing the capture rule with the correction growth of MC method, if the liquid cell is not captured by the judgement of CA technique, the further judgement is done by MC method. The growth probability for the liquid cell, $P_g(x, y, t + \Delta t)$ can be calculated as follows

$$P_g(x, y, t + \Delta t) = \begin{cases} 0 & \Delta T \leq 0 \\ \exp\left(\frac{-\Delta F_g(x, y, t + \Delta t)}{k_b T}\right) & \Delta T > 0 \end{cases} \quad (18)$$

$$\Delta F_g = \Delta F_v + \Delta F_s$$

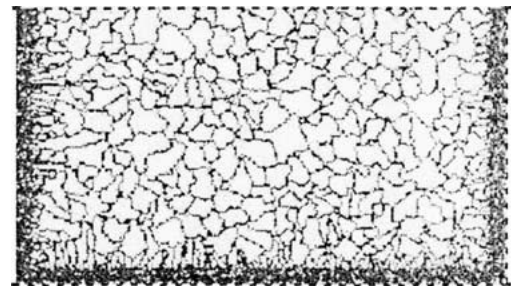


Figure 8 Solidification structures simulated by CA/MC model.

where ΔF_g is the change of free energy, ΔF_v is the change of bulk free energy, ΔF_s is the interfacial energy, and k_b is the Boltzmann constant.

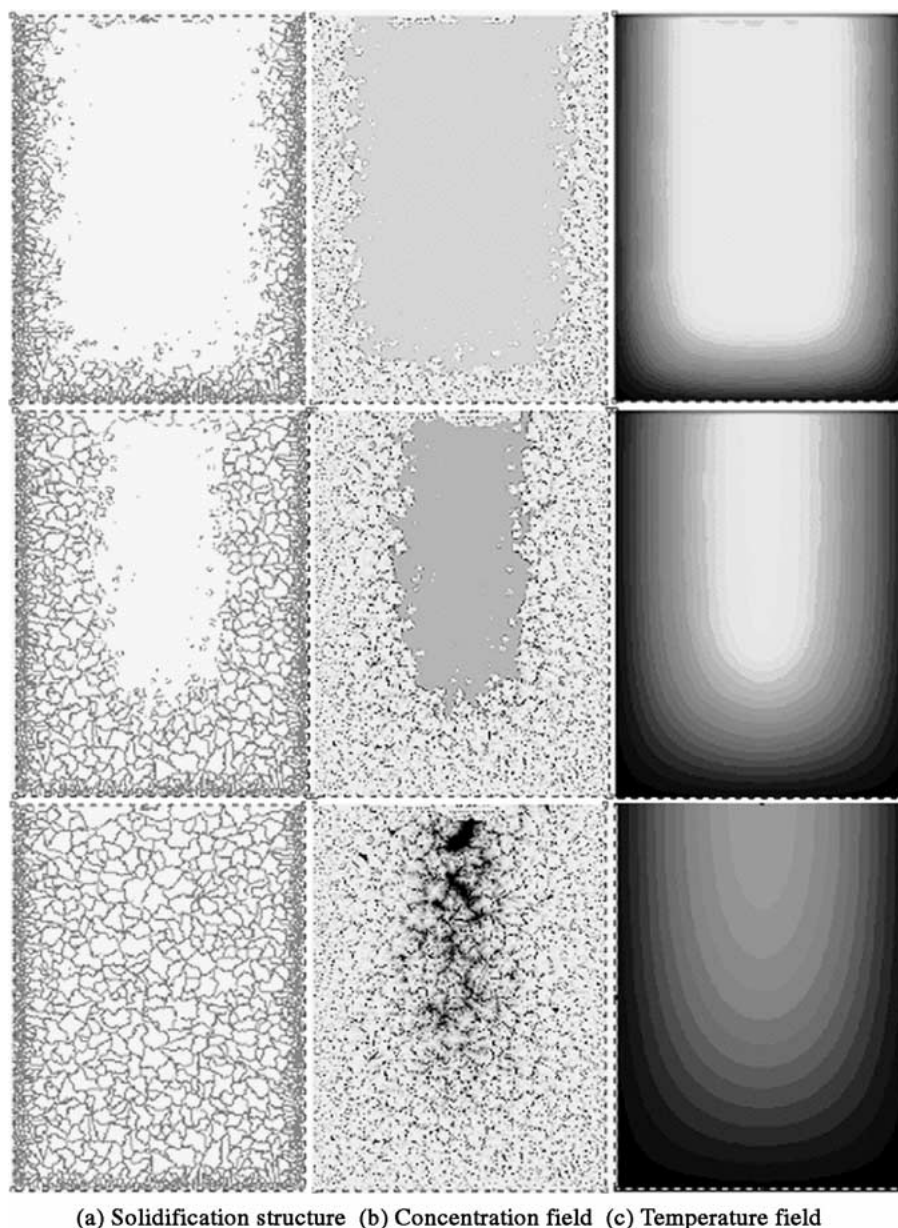
Then, the similar random procedure as nucleation will be treated for the liquid cell. If $p_g > r$, r is a random number ($0 \leq r \leq 1$), the cell's growth also succeeds.

In order to keep the CA technique leading status in the simulation of grain growth, the area for MC correction growth has to be limited, as shown in Fig. 6 (represented by dashed circle).

The model combining CA technique and MC method is called CA/MC model here. The grain images simulated by using CA/MC model are shown in Fig. 7. It is noted that the results are better agreement with experimental observation than that of Fig. 5. Accordingly, the solidification structures simulated by CA/MC model are shown in Fig. 8. The amount, size and appearance of grains can be seen more clearly compared with the results only by CA technique or MC method.

6. Results and discussion

Fig. 9 shows the evolution of the grain structures, concentration field and temperature field during



(a) Solidification structure (b) Concentration field (c) Temperature field

Figure 9 The formation of solidification structures simulated by CA/MC model.

solidification, which are simulated by the CA/MC model, the Actual Solute Partition Coefficient model and the Alternant Explicit Difference method respectively. The two-dimensional ingot of Al-4.5% (mass) Cu alloy corresponds to $5 \times 6 \text{ cm}^2$ billet cast in a cooling-water Cu mould with cooling water flux 170 ml/min. The experimental observations of solidification structures is shown in Fig. 10.

In Fig. 9a, at the beginning of solidification, a lot of nuclei are formed at the surface of mould because of the chilling of cool water. These nuclei have random orientations. As growth proceeds, only those grains with their $\langle 10 \rangle$ crystallographic orientation most closely aligned with the normal to the mould surface are selected to form columnar grains, and this selection mechanism is well reproduced by the CA technique. The growth of these columnar grains is quickly restrained by the equiaxed grains formed largely in the centre of the ingot due to the rapid increase of undercooling. Therefore, the underdevelopment columnar grains are finally obtained. And that equiaxed grains



Figure 10 The final solidification structures of Al-4.5% (mass) Cu alloy in water-cooling Cu mould.

grow further according to the branching mechanism which is reflected by MC method adequately. It is obvious that the formation of solidification structures can be simulated well by the CA/MC model. Compared with the final solidification structures of experiment

as shown in Fig. 10, the simulation results are believable.

In Fig. 9b, it is noted clearly that the solutes are enriched in the solid/liquid interface, and the solute segregation occurs in grain and boundary. As growth proceeds, more and more solute are separated in the front of interface, so that abundance solutes are left in the final solidification area.

Fig. 9c shows the corresponding temperature field.

7. Conclusions

1. The Actual Solute Partition Coefficient model is established to calculate the solute redistribution of solid/liquid interface, which is based on the simulation of solidification structures. The segregation in grain and boundary can be simulated well by this model.

2. By combining the CA technique and MC method, develop the CA/MC model for the first time. By using the model, the evolution of amount, size and appearance of grains can be simulated better than the results only by CA technique or MC method.

3. The solidification structures simulated by using CA/MC model are well agreement with the results obtained experimentally.

Acknowledgement

The authors gratefully acknowledge the support of the National Nature Science Foundation of China (No. 59995442) and the National Key Fundamental Research of China (No. G1998061500).

References

1. C. Y. WANG and C. BECKERMANN, *Metall. Mater. Trans.* **25A** (1994) 1081.
2. *Idem.*, *ibid.* **27A** (1996) 2754.
3. *Idem.*, and *ibid.* **27A** (1996) 2765.
4. J. A. SPITTLE and S. G. R. BROWN, *Acta Metall.* **37** (1989) 1803.
5. PANPING ZHU and R. W. SMITH, *ibid.* **40** (1992) 683.
6. *Idem.*, *ibid.* **40** (1992) 3369.
7. M. RAPPAZ, and CH.-A. GANDIN, *ibid.* **41** (1993) 350.
8. CH. CHARBON, and M. RAPPAZ, *ibid.* **42** (1994) 2233.
9. J. A. BUTTON, R. C. PRIM and W. G. SLICHTER, *J. Chem. Phys.* **21** (1953) 1987.
10. M. J. AZIZ, *J. App. Phys.* **53** (1982) 1158.
11. I. STEINBACH, C. BECKERMANN, B. KAUEAUF, Q. LI and J. GUO, *Acta Metall.* **47** (1999) 971.

Received 22 September 2000

and accepted 11 December 2001